Lukas Bernauer BSc

Cell Wall Integrity pathways in *Pichia pastoris*

MASTER'S THESIS

to achieve the university degree of

Diplom-Ingenieur

Master's degree programme: Biotechnology

submitted to

Graz University of Technology

Supervisor

Dipl.-Ing. Dr. techn. Anita Emmerstorfer-Augustin

Assoc. Prof. Dipl.-Ing. Dr. techn. Harald Pichler

Institut für Molekulare Biotechnologie, Technische Universität Graz

Graz, März 2020

AFFIDAVIT

EIDESSTATTLICHE ERKLÄRUNG

Ich erkläre an Eides statt, dass ich die vorliegende Arbeit selbstständig verfasst, andere als die angegebenen Quellen/Hilfsmittel nicht benutzt, und die den benutzten Quellen wörtlich und inhaltlich entnommenen Stellen als solche kenntlich gemacht habe. Das in TUGRAZonline hochgeladene Textdokument ist mit der vorliegenden Masterarbeit identisch.

_____   _____

Datum   Unterschrift

Danksagung

Ich möchte mich bei folgenden Personen vielmals für ihre Beteiligung an der Entstehung dieser Arbeit bedanken:

- Anita Emmerstorfer-Augustin für ihre hervorragende Betreuung meiner Arbeit
- Meinem Arbeitsgruppenleiter Harald Pichler für Motivation und Rat während der Zeit im Labor
- Barbara Schwarzbauer für ihre hervorragende Hilfe im Labor
- Heimo Wolinski für seine großartige Hilfe bei der Durchführung der Fluoreszenzmikroskopie
- Christoph Augustin für seine unschätzbare Hilfe bei der Datenauswertung der Mikroskopiebilder
- Meinen Arbeitsgruppenkollegen Isa, Tamara, Jan, Jürgen, Hannes, Sandra, Matthias, Lhamo, Myria und Simon für das wunderbare Arbeitsklima und die stetige Unterstützung während der Arbeit
- Und natürlich bei meinen Eltern, die das Studium ermöglicht haben und meinen Geschwistern, die stets für mich da waren

Table of contents

Abstract

Sterols are important lipids found in the plasma membrane (PM) of all eukaryotic cells. In this study, we made use of an engineered *P. pastoris* strain that produces mammalian cholesterol instead of its native ergosterol. Exchange of ergosterol for cholesterol causes upregulated cell wall biosynthesis in the cell, a phenomenon never observed before. In order to investigate, which membrane proteins upregulate cell wall biosynthesis in response to sterol modifications, we compared the role of cell wall integrity (CWI) proteins in a wild type and cholesterol producing strain. CWI proteins are stress sensors in the fungal plasma membrane and reach into the cell wall. Activation of CWI proteins initiate a MAP kinase cascade, which leads to the regulation of genes responsible for cell wall synthesis and cell cycle progression. Upon blasting the known sequences of CWI proteins from *S. cerevisiae* against the *P. pastoris* genome, we identified the loci of *WSC1, WSC2* and *WSC3,* whereas no homologs of Mlt2 and Mid1 could be found.

To investigate the role of Wsc1, Wsc2 and Wsc3 in initiating cellular stress response, we knocked out the corresponding genes in a *P. pastoris* wild type and cholesterol strains. The cholesterol producing strain showed growth defects and decreased resistance to stressful conditions. Wsc knockout mutants, however, did not exhibit any further changes in growth behaviour as shown by spot assays. To also visualize the localization and cellular abundance, we tagged Wsc2 and Wsc3 with mNeonGreen, an extremely bright fluorescent protein. While very little Wsc2 seemed to be expressed, Wsc3-mNG could be readily detected at the cell periphery. Wsc3 clearly accumulated at the plasma membrane in cholesterol producing strains which may explain the upregulation of cell wall biosynthesis.

Zusammenfassung

Sterol sind wichtige Lipide, die man in der Plasmamembran aller eukaryotischer Zellen findet. In dieser Studie verwenden wir einen modifizierten *P. pastoris* Stamm, der anstatt des nativen Ergosterols Cholesterol produziert. Der Austausch von Ergosterol zu Cholesterol führt zu einer Hochregulierung der Zellwandbiosynthese, ein Phänomen, das nie zuvor beobachtet wurde. Um zu untersuchen, welche Membranproteine, im Zuge der Sterolmodifizierung die Zellwandbiosynthese hochregulieren, verglichen wir die Rolle der cell wall integrity (CWI) Proteine in einem Wildtyp- und einem Cholesterol produzierendem Stamm. CWI Proteine sind Stresssensoren in der Plasmamembran von Hefen und reichen in die Zellwand. Aktivierung von CWI Proteinen initiiert eine MAP-Kinasekaskade, welche die Regulierung von Genen verantwortlich für Zellwandsynthese und Fortschreiten des Zellzyklus, einleiten. Durch Blasten der bekannten Sequenzen von CWI Proteinen aus *S. cerevisiae* gegen das Genom von *P. pastoris,* konnten wir die Loci von *WSC1*, *WSC2* und *WSC3* identifizieren. Es konnten keine Homologe zu Mlt2 und Mid1 ausfindig gemacht werden.

Um die Rolle von Wsc1, Wsc2 und Wsc3 in der Einleitung der zellulären Antwort auf Stress zu untersuchen, schalteten wir die jeweiligen Gene in einem *P. pastoris* Wildtyp und einem Cholesterol Stamm aus. Der Cholesterol produzierende Stamm zeigte Defekte beim Wachstum und eine reduzierte Resistenz gegen Stress. Mutanten mit ausgeschaltetem *WSC* zeigten aber keine weiteren Veränderungen in ihrem Wachstumsverhalten. Um die Lokalisierung und Menge von Wsc2 und Wsc3 zu visualisieren, fusionierten wir die jeweiligen Proteine mit mNeonGreen, einem sehr hellen, fluoreszierenden Protein. Während scheinbar nur sehr wenig Wsc2 exprimiert wird, konnte Wsc3-mNG leicht in der zellulären Preipherie detektiert werden. Wsc3 akkumulierte eindeutig in der Plasmamembran von Cholesterol produzierenden Stämmen, was die Hochregulierung der Zellwandbiosynthese erklären könnte.

Introduction

Fungal cell walls give cells mechanical stability and are essential for survival. The cell wall consists of carbohydrates and mannoproteins, which are linked with chitin chains. There are many different cell wall proteins, which are required for several functions, including cell division, cell fusion during the mating process and the dynamic remodelling of the cell wall (1).

In its role as the first contact point of the fungal cell with its environment, the cell wall is also confronted with different stresses, for example changes in pH or osmolarity. In yeast, some of these environmental changes are detected by cell wall integrity (CWI) proteins, which trigger a signal transduction cascade, initiating the cellular response (2). In *S. cerevisiae*, which has predominantly been used to study the CWI pathway, we find five CWI proteins, Wsc1, Wsc2, Wsc3, Mid2 and Mtl1 (3). *WSC* knock-out mutants were shown to be more sensitive to certain environmental stress conditions, for example heat and to develop a hypersensitivity for ethanol (4).

While the overall pathway seems to be conserved in all yeasts, there have only been little efforts to study the CWI pathway in alternative yeasts in more detail. All Wsc proteins have a very similar structure. They have a cysteine-rich head group, which is supposedly in contact with the cell wall glucans, followed by an O-mannosylated serine/threonine rich (STR) region, a spring-like structure, that reaches into the cell wall. A single transmembrane domain connects the protein with its cytoplasmic domain. The cytoplasmic domain interacts with the downstream enzyme pathway and also carries a signal, which is important for internalization and degradation of the protein and, therefore, the tempering of the stress response. Mutation of the endocytic signal negatively influences cell growth, whereas the cell wall becomes thicker than usual (5,6).

S. cerevisiae encodes another gene similar to the already mentioned *WSC*-genes, namely *WSC4.* The protein Wsc4 is supposed to have a similar structure as the other Wsc variants and is also involved in cellular stress response. However contrary to the other Wsc proteins it is located at the membrane of the endoplasmic reticulum and its functions overlap only partially with Wsc1, 2 and 3. It is responsible for the translocation of soluble secretory proteins and the insertion of membrane proteins into the ER membrane. It has also been proposed as a viable target for strain improvement

towards secretion of recombinant proteins in *Pichia pastoris* (7–9). However, since it being not directly related to the yeast cell wall it was not further studied here.

Stress-induced activation of the CWI pathway causes Wsc proteins to aggregate in the plasma membrane and their cytoplasmatic domains to interact with the GDP/GTP exchange factor Rom2. Rom2 activates the GTPase Rho1 by exchanging the coupled nucleotide. This activates Pkc1, a yeast protein kinase, which in turn leads to the activation of a mitogen-activated protein kinase (MAPK) cascade, with its final MAP kinase Slt2 being phosphorylated. Phosphorylated Slt2 is shuttled to the nucleus where it initiates gene expression, targeting for example transcription factors, which regulate cell cycle progression and cell wall synthesis. Mutants with disrupted Slt2 have been reported to show increased sensitivity to higher temperature and certain cell-wall destabilizing compounds, e.g. caffeine (10,11).

Sterols are a class of lipids, that are important for the regulation of different processes and the integrity of domain structures in biological membranes (12). They are necessary for the formation of so called 'lipid-rafts', which are needed for different biological functions such as signal transduction, cellular sorting, cytoskeleton reorganization and others. Further, they are needed to maintain the fluidity of membranes, especially at extreme temperatures (13,14). The major phylogenetic kingdoms all possess their own specific sterols. While we find different sterols in plants, e.g. stigmasterol and sitosterol, the major sterol in mammals is cholesterol, and in fungi ergosterol. Due to the fact that these sterols share common precursor molecules, e.g. cholesta-5,7,24(25)-trienol, it is rather easy to create a yeast strain that produces cholesterol instead of ergosterol (15).

Therefore ergosterol-synthesis genes *ERG5* and *ERG6* need to be replaced by dehydrocholesterol reductases *DHCR7* and *DHCR24* were, respectively (16) (Figure 1).
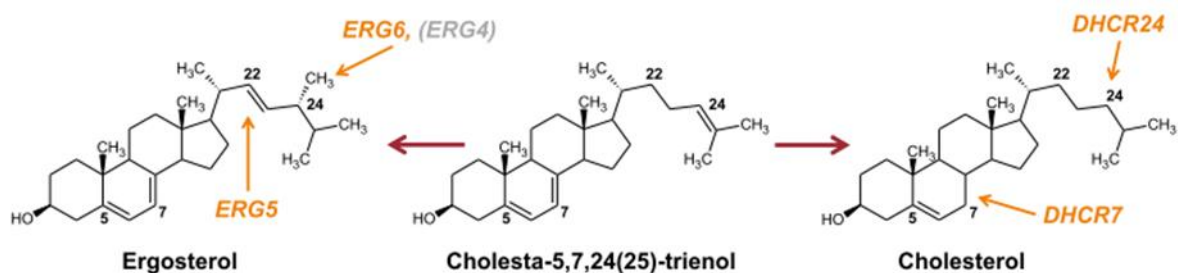
Figure 1: **Synthesis of ergosterol and cholesterol from their common precursor molecule cholesta-5,7,24(25)-trienol in their respective organisms.** (16)

In the past, cholesterol producing *P. pastoris* strains have successfully been used to improve expression of human membrane proteins, which need to tightly bind cholesterol for proper stability (16). Even though cholesterol and ergosterol display high structural similarity, they cannot simply be interchanged in their host organism without severely disturbing a diverse range of cell-membrane associated mechanisms.

In the course of further strain characterization, it was found that the cholesterol producing strains had severe growth defects, especially at low temperatures and decreased resistance to certain harmful compounds. Electron microscopy images revealed that the exchange of ergosterol for cholesterol forced cells to produce thicker, amorphous cell walls (Figure 2).
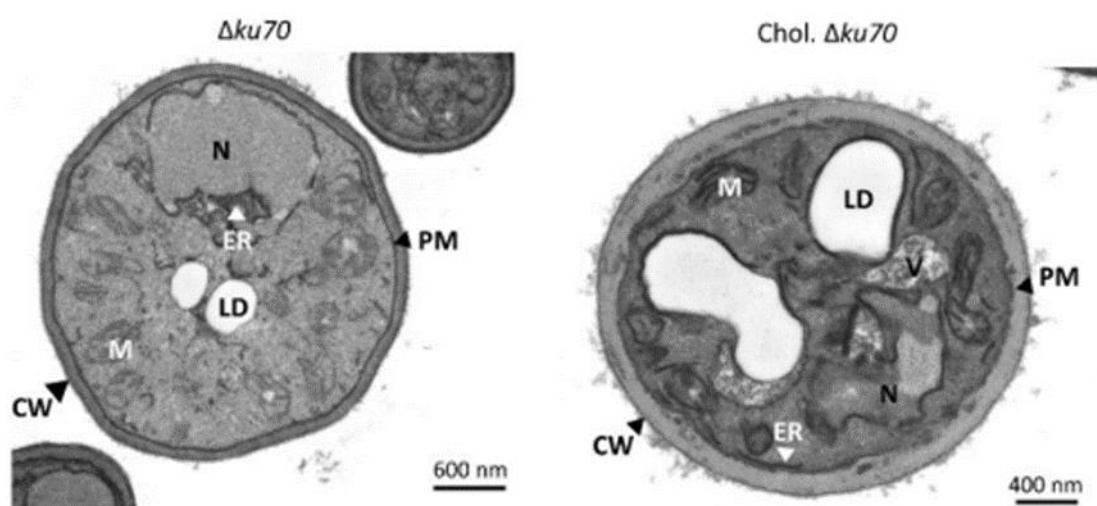
Figure 2: **EM images of *P. pastoris.*** Native ergosterol producing cell (left) and cholesterol producing cell (right). The cell wall of the cholesterol strain is thicker than the native cell wall and irregular. Cells were grown for 48 h in YPD medium. ER – endoplasmic reticulum; N – nucleus; PM – plasma membrane; LD – lipid droplet; M – mitochondria; CW – cell wall. Figure from (17)

Cholesterol producing strains also display continuously upregulated phosphorylation of Pim1p, the *P. pastoris* homologue of Slt2, indicating activation of the CWI pathway in these strains (17). Since the CWI pathway is involved in cell wall synthesis and cell propagation, functions which are both disturbed in the cholsterol producing *P. pastoris* cells, these strains were selected to investigate the role of Wsc1, Wsc2 and Wsc3 in sensing and signaling the presence of non-native cholesterol.

Material and Methods

The instruments and reagents used, are described in the Appendix.

Cloning and strain construction

All plasmids used in this study were generated using Gibson assembly (18). Primer used are summarized in Table S 5. PCR amplification was performed using Phusion DNA polymerase (New England BioLabs, Ipswich, MA), and all constructs were verified by DNA sequencing. Correct integration of expression cassettes into the yeast genome were confirmed by colony PCR and sequencing. Transformation of *P. pastoris* was done according to the condensed protocol of Lin-Cereghino et al. (19). Cells were transformed with 0.5 µg of linearized DNA and regenerated for 1 h in 0.5 mL of 1 M sorbitol and 0.5 mL of YPD medium. The cell broth was then plated onto MD agar lacking histidine for selection.

Genomic DNA isolation from *P. pastoris* for colony PCR

As described by Looke et al. (20), a small cell pellet was resuspended in 100 µL of 1% SDS and 0.2 M lithium acetate. The mixture was incubated for 10 min at 65°C. Afterwards, 300 µL of 96% ethanol were added and the whole mixture was centrifuged for 3 min at 13,000 rpm. After removal of the supernatant, the pellet was washed with 500 µL of 70% ethanol and was resuspended in 70 µL of ddH$_2$O. 1 µL of isolated DNA was used as a template for colony PCR.

Knock-out and fluorescence tagging strategy for Wsc-proteins in *P. pastoris*

To knock out *WSC1, 2 and 3* and to C-terminally tag *WSC2* and *WSC3* with mNeonGreen, homologous regions of respective genes, and genes fused to mNeonGreen, respectively, were cloned up- and downstream of the *HIS4* marker of pPpKC3 (21) and flanked by blunt-end *Smi*I restriction sites (Figure S 2). *WSC* knockout and mNeonGreen knockin cassettes were cut out of pPpKC3 using *Smi*I, purified and used for transformation.

Spot assays

P. pastoris strains were grown overnight in 5 ml of YPD medium. Strains were diluted to an OD$_{600}$ of one, and five-fold serial dilutions were prepared in sterile 96-well plates.

Cells were replica-plated on YPD or MD (containing histidine) plates with and without 10 mg/L calcofluor white (CFW), 1 M sorbitol, or both. Experiments were done in duplicates and plates were incubated for two days at 30°C, or 20°C.

Sterol analysis

Sterol analysis of *P. pastoris* was performed as described in Quail and Kelly (22) with minor modifications. Cell cultures were grown for 15 or 40 h in YPD medium at 30°C. Sterols were extracted from 15 OD_{600} units of cells. The cell pellets were resuspended in 1 mL of 0.2 % pyrogallol in methanol and 0.4 mL of 60% aqueous KOH solution. The samples were incubated at 90°C for 2 h. Afterwards they were cooled down and 1 mL of n-heptane was added. The samples were mixed at 1500 rpm for 3 min and then centrifuged at 2500 rpm for another 3 min. The upper phase was transferred to a fresh tube and the extraction step was repeated. The extracts were dried under nitrogen steam. The extracted sterols were dissolved in 10 µL of pyridine and derivatized with 50 µL of N'O'-bis(trimethylsilyl)-trifluoroacetamide for 10-20 min. 200 µL of ethyl acetate were added and the samples were analysed by gas chromatography – mass spectrometry (GC-MS) as described in Ott et al. (23). Compounds were identified based on their mass fragmentation pattern and their retention time. A quick test towards ergosterol production was also done by streaking clones on YPD-agar plates containing 50 mg/mL natamycin.

Cell disruption by Riezman protocol

Cells were disrupted for further protein analysis using immunoblotting. Cell cultures were grown for 15 h in YPD medium at 30°C. 5 OD_{600} units of cells were collected for disruption. All steps were performed at 4°C. Cell pellets were resuspended in 300 µL of 1.85 M NaOH containing 7.5% β-mercaptoethanol. The samples were incubated at 4°C for 10 min, then 300 µL of 50% trichloroacetic acid were added, and the samples were again incubated at 4°C for 1 h. Afterwards, the samples were centrifuged for 5 min at 10,000 rpm. After discarding the supernatant, the pellets were washed with 0.5 mL of ice cold ddH_2O and resuspended in 100 µL of sample buffer (16.5 µL of NuPage LDS Sample Buffer, 33 µL of 1 M Tris-Base, 2 µL of β-mercaptoethanol and 49.5 µL of ddH_2O). The samples were centrifuged at 7,000 rpm for 1 min to remove cell debris and 15 µL of extracted protein could be used for SDS-PAGE.

Cell disruption with glass beads

Cell cultures were grown for 15 h in YPD medium at 30°C. 5 OD_{600} units of cells were used for disruption. The cell pellet was resuspended in 250 µL Buffer A and glass beads (d: 0.25-0.5 mm) were added. The samples were ten times alternatingly vortexed for 30 s and cooled on ice for 30 s. Afterwards the samples were centrifuged at 13,000 rpm for 1 min and the supernatant was used for protein concentration measurement. Protein concentrations were measured with the "BCA™ Protein Assay Kit". All measurements were done in duplicates.

Immunoblot analysis

SDS-PAGE and blotting of gels was performed according to the manual of the Mini Gel Tank from Thermo Fisher Scientific. 15 µL of protein extracts or 20 µg of protein acquired by glass bead disruption were loaded onto the gel. The protein mixtures were denatured at 70°C for 10 min prior to loading. 5 µL of PageRuler™ Prestained Protein ladder were used as standard. The gels were run in MOPS SDS Running Buffer at 200 V and 80 mA for 50 min. After gel electrophoresis, the proteins were blotted onto a nitrocellulose membrane. The blotting was done in transfer buffer (see Table S 3) at 10 V for 1.5 h. Afterwards, membranes were stained with PonceauS and scanned. Membranes were destained with TBST and blocked with 5 % bovine serum albumin (BSA) in TBST for 1 h at moderate shaking and room temperature. Blocked membranes were incubated at 4°C overnight with the appropriate antibodies. Phosphorylated Pim1 was detected by Phospho-p44/42 MAPK (Erk1/2) (Thr202/Tyr204) antibody (1:5000 dilution in TBST with 5% BSA) (Cell Signaling Technology®) and Wsc proteins fused to mNeonGreen by HA-Tag (6E2) Mouse mAb (HRP Conjugate) (1:2500 dilution in TBST with 2.5% milk powder) (Cell Signaling Technology®). Then, they were washed five times with 50 mL TBST for 5 min at moderate shaking and the secondary antibody (Anti rabbit IgG, 1:1000 dilution in TBST with 2,5% milk powder) was applied. HA-tags were detected with an anti-HA antibody conjugated to HRP. After another five washing steps, the ECL substrate for horse radish peroxidase was applied according to the Clarity Max™ Western ECL Substrate from Bio-Rad and the signal detected for 1-10 min in the G:Box Supreme. Band intensities were quantified using the ROI manager tool from Fiji (24). Signal strength was normalised, using the scan from PonceauS stained membrane.

Fluorescence microscopy

Cells were diluted to an OD_{600} of 0.1 and grown in minimal medium containing histidine until they reached an OD_{600} of 2. Microscopy was performed on a Leica SP5 confocal microscope (Leica Microsystems Inc., Germany) and using a 63x, NA 1.4 HCX PL APO oil immersion objective. mNeonGreen was excited at 488 nm and emission was detected between 500-550 nm. Fluorescence and transmission images were acquired simultaneously. Images shown in one Figure were taken the same day to avoid differences in laser intensity. Cells were segmented manually using Fiji software and the intensity of the fluorescence signal was quantified using a CellProfiler pipeline (25).

Results and Discussion

Homologous genes of the major key players of the CWI pathway exist in *P. pastoris*

Performing a BLAST search with sequences of the core proteins of the CWI pathway in *S. cerevisiae* against the *P. pastoris* CBS7435 genomic sequence showed that homologous proteins of the pathway are present (Table 1). Interestingly, no homologous proteins could be found for Mid2 and Mtl1 in *P. pastoris*.

Table 1: **Proteins of the CWI pathway found in *S. cerevisiae* and their homologs in *P. pastoris*. Results of BLASTp searches are shown and values represent homology to the closest *P. pastoris* homolog(s).**

Protein in *S. cerevisiae* (systemic name)	Protein in *P. pastoris* CBS7435 (protein ID, chromosome number)	Protein BLAST (query covery/E-value/Ident)
Wsc1 (YOR008C)	Wsc1 (CCA39485.1, chromosome 3)	35% / 6e-14 / 37%
Wsc2 (YNL283C)	Wsc3 (CCA37334.1, chromosome 1)	61% / 1e-16 / 37%
	Wsc2 (CCA37335.1, chromosome 1)	18% / 3e-09 / 32%
Wsc3 (YOL105C)	Wsc3 (CCA37334.1, chromosome 1)	19% / 2e-18 / 37%
	Wsc2 (CCA37335.1, chromosome 1)	16% / 2e-07 / 28%
Rho1 (YPR165W)	Rho1 (CCA40030.2, chromosome 3)	94% / 5e-105 / 70%
Rom2 (YLR371W)	Rom2 (CCA39932.1, chromosome 3)	80% / 1e-126 / 37%
Pkc1 (YBL105C)	Pkc1 (SCV12115.1, chromosome 2)	78% / 0.0 / 54%
Slt2 (YHR030C)	Pim1 (CCA39249.1, chromosome 3)	74% / 0.0 / 67%

Based on homology searches, a schematic of the core elements of the CWI pathway was adapted to the proteins found in *P. pastoris* and is presented in Figure 3.
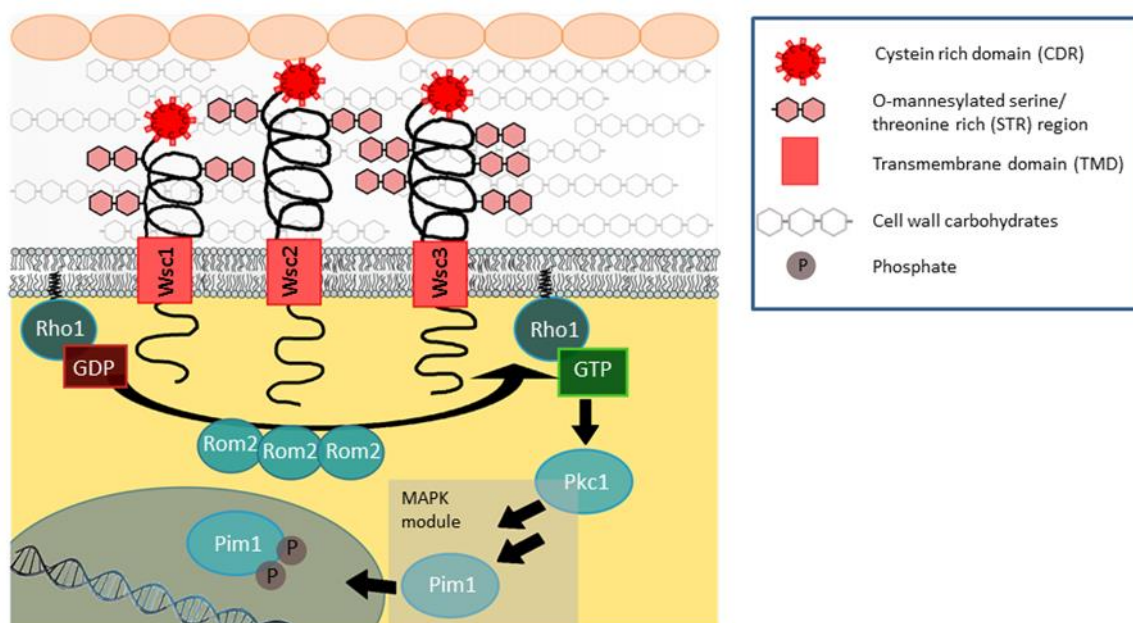
Figure 3: **Schematic representation of the CWI proteins and their corresponding pathway in *P. pastoris.*** CWI proteins exhibit several highly conserved domains, including the CDR head group, the STR region and the transmembrane domain with the cytoplasmic region. The cytoplasmic region interacts with Rom2, which exchanges the coupled nucleotide of the GTPase Rho1. This activates the MAPK cascade, which leads to phosphorylation of Pim1 and the regulation of gene expression corresponding to cell wall synthesis and cell cycle progression. Figure kindly provided by Anita Emmerstorfer-Augustin

Sterol analysis of wild type and cholesterol producing strains

In order to confirm biosynthesis of the correct sterol (ergosterol in wild type strains and cholesterol in engineered strains), sterol analysis was done for all strains used in this study. We first tested growth of wild type and cholesterol producing strains on agar plates containing 50 mg/mL natamycin. Natamycin is an antibiotic that binds specifically to ergosterol and, thereby, inhibits fungal growth (26). Based on the fact that strains expressing cholesterol instead of ergosterol should be resistant to this drug, we expected to be able to distinguish between cells producing ergosterol and cholesterol. However, strains only producing precursors of cholesterol were also resistant to natamycin. Hence, in order to provide very clear data, which sterols are produced, GC-MS analyses were performed. As expected, wild type cells predominantly produced ergosterol and engineered strains predominantly produced cholesterol. However, we noticed a difference when cells were harvested at different time points. After 15 h of growth at 30°C in YPD, cholesterol producing strains contained about 60 % cholesterol and another sterol variant, most likely 7-dehydrocholesterol, a precursor molecule of cholesterol (Figure 4). After 40 h of

growth, however, overall cholesterol contents increased to roughly 90 %. The delay in the production of cholesterol may be due to lower activity of *DHCR7* and *DHCR24* in *P. pastoris* at an early growth phase. Further, there is no real advantage for the cell in producing cholesterol from its precursor, e.g. 7-dehydro-cholesterol, since both are non-native sterols and negatively influence cell growth (16).
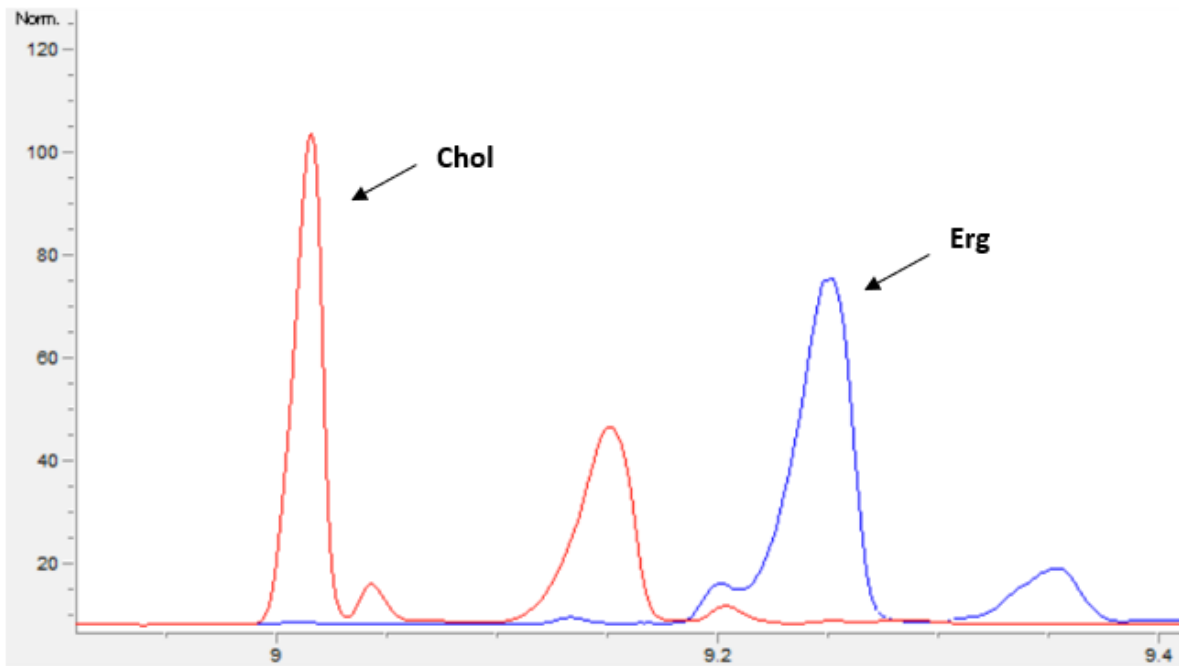

Figure 4: **Cholesterol strains contain 60 % cholesterol after 15 h growth.** CBS7435 (blue) and cholesterol strain (red, MH458) were grown for 15 h at 28°C in YPD. Sterol composition of the whole cell was analysed as described in Materials and Methods. Peaks for cholesterol and ergosterol were marked.

Cholesterol producing strains are more sensitive to growth on cell-disturbing reagents and at low temperatures

In order to examine the impact of sterol perturbations on cellular growth under certain conditions such as low temperature, or the addition of cell wall disturbing (e.g. calcofluor white (CFW)) and cell wall stabilising reagents (sorbitol), spot assays were performed. To additionally investigate the role of CWI proteins in responding to these conditions, we knocked out *WSC1*, as well as *WSC2* and *WSC3* in *P. pastoris* CBS7435 wild type and cholesterol producing strains. *WSC2* and *WSC3* could be knocked out simultaneously due to their very close proximity in the genome (27). Table 2 gives an overview of all strains used in this study.

Table 2: **List of *P. pastoris* strains used in this study**

Name	Description	Source
CBS7435	CBS7435 *his4Δ*	(28)
MH458	CBS7435 *his4Δ erg5Δ::DrDHCR7*-Zeo^R *erg6Δ::DrDHCR24*-G418^R	(16)
yLB118	CBS7435 *his4Δ wsc1Δ::HIS4*	This study
yLB121	CBS7435 *his4Δ wsc2-3Δ::HIS4*	This study
yLB124	CBS7435 *his4Δ erg5Δ::DrDHCR7*-Zeo^R *erg6Δ::DrDHCR24*-G418^R *wsc1Δ::HIS4*	This study
yLB127	CBS7435 *his4Δ erg5Δ::DrDHCR7*-Zeo^R *erg6Δ::DrDHCR24*-G418^R *wsc2-3Δ::HIS4*	This study
yLB130	CBS7435 *his4Δ WSC2-mNG-HA HIS4*	This study
yLB133	CBS7435 *his4Δ WSC3-mNG-HA HIS4*	This study
yLB136	CBS7435 *his4Δ erg5Δ::DrDHCR7*-Zeo^R *erg6Δ::DrDHCR24*-G418^R *WSC2-mNG-HA HIS4*	This study
yLB139	CBS7435 *his4Δ erg5Δ::DrDHCR7*-Zeo^R *erg6Δ::DrDHCR24*-G418^R *WSC3-mNG-HA HIS4*	This study

All strains producing cholesterol exhibited reduced growth at 20°C on plates, irrespective of whether Wsc proteins had additionally been knocked out (Figure 5A). Also, cholesterol producing strains were more sensitive to the cell wall disturbing reagent CFW (Figure 5B). This is not surprising, since earlier studies have shown that cholesterol producing strains exhibit a thicker cell wall, which allows CFW to interact with a much bigger surface (17), (Figure 2). Based on the fact that cholesterol producing strains and/or *wscΔ* mutants (5) may be less stable due to cell wall defects, we additionally grew cells on 1 M sorbitol for osmotic stabilization. However, we did not notice any significant difference in growth (Figure 5C).
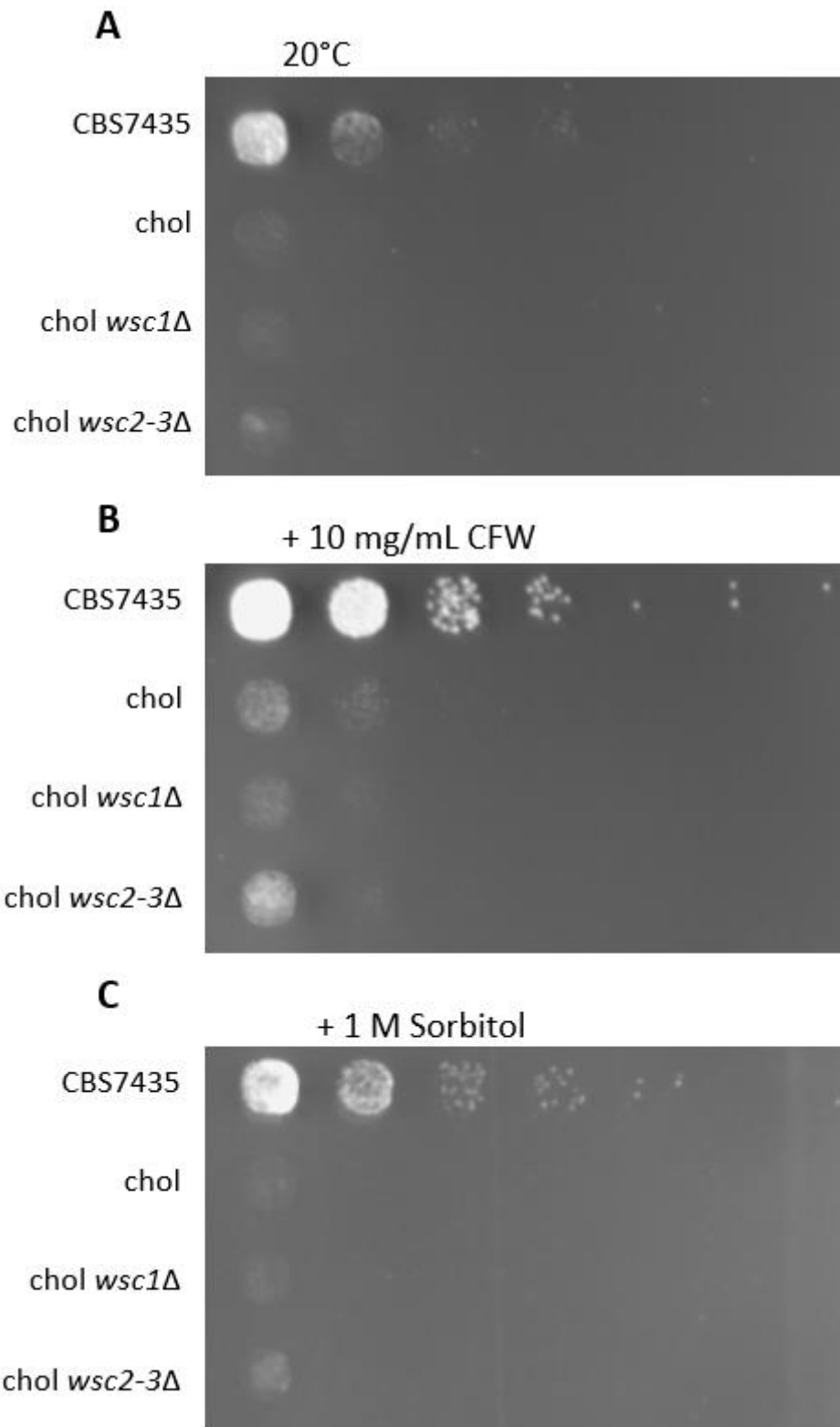
Figure 5: **Spot assays for strains CBS7435, CBS7435 cholesterol (MH458), CBS7435 cholesterol *wsc1*Δ (yLB124) and CBS7435 cholesterol *wsc2-3*Δ (yLB127) grown on (A) MD+histidine plates at 20°C, (B) MD+histidine plates containing 10 mg/ml CFW at 28°C, or (C) MD+histidine plates containing 1 M sorbitol at 28°C.**

Examining the role of Wsc proteins in activating the CWI pathway in cholesterol producing strains

From previous studies we know that Pim1 is hyperphosphorylated in cells producing cholesterol instead of ergosterol (16). Since it is known that the Wsc-proteins activate the MAPK-cascade, which ultimately leads to phosphorylation of Pim1, we tested Pim1 phosphorylation in our *wsc*Δ knockout strains.

While all cholesterol strains still produced significantly more phosphorylated Pim1 than wild type strains, no difference in Pim1 phosphorylation could be observed in case *WSC1* or *WSC2* and *WSC3* were knocked out (Figure 6).

A possible reason could be that Wsc1, Wsc2 and Wsc3 are biologically redundant and all required to properly respond to changes in sterol patterns by activating the CWI pathway. Unfortunately, our attempts to generate a triple knockout failed, which strongly hints at synthetic lethality. It may also be possible that another pathway crosstalks with the CWI pathway, and thereby, upregulates Pim1 phosphorylation in cholesterol producing *P. pastoris*, e.g. TORC2 signalling (29).
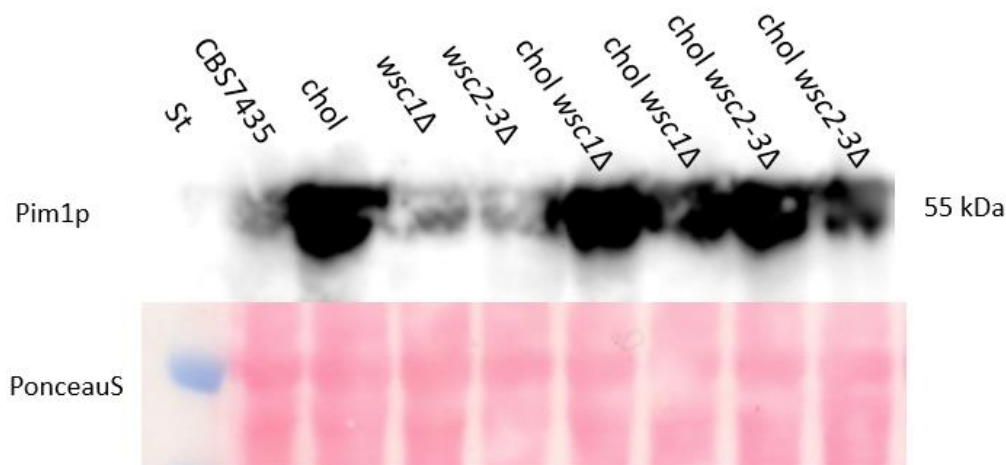
Figure 6: **Pim1 hyperphosphorylation in strains producing cholesterol.** Wild type cells (CBS7435), otherwise isogenic *wsc1*Δ (yLB118) and *wsc2*Δ *wsc3*Δ (yLB121) single mutant derivatives, as well as CBS7435 strains producing cholesterol (MH458) and otherwise isogenic *wsc1*Δ (yLB124) and *wsc2*Δ *wsc3*Δ (yLB127) single mutant derivatives were grown for 40 h at 28°C in YPD, harvested, and lysed. Total cell lysates were resolved by SDS–PAGE and analysed by immunoblotting with anti-phospho-p44/42 antibody, as described under Materials and Methods. Loading control, PonceauS.

WSC2 and *WSC3* are expressed at different levels in wild type and cholesterol strains

To investigate the cellular localization and abundance of CWI proteins, we tagged Wsc2 and Wsc3 with mNeonGreen (mNG). mNG is a monomeric green-fluorescent protein, derived from *Branchiostoma lanceolatum* and, therefore, not a variant of the common GFP. It was reported to be up to three times brighter than GFP, using the same filter sets (30). All proteins were additionally tagged with an HA-tag to facilitate detection of the respective proteins by immunoblot analysis.

Immunoblot detection of Wsc2-mNG and Wsc3-mNG showed extremely low expression levels of Wsc2-mNG (Figure 7A). Fluorescence microscopy additionally confirmed that Wsc2 was barely detectable in neither the wild type, nor the cholesterol producing strain (Figure 7B). Wsc3, however, was expressed at high rates. As mentioned above, both genes are located next to each other in the *P. pastoris* genome, whereas the *WSC2* ATG-start codon is placed almost immediately after the *WSC3* TAA-stop codon, providing it only with an extremely short promoter region. This might explain the low expression level of Wsc2. In *S. cerevisiae*, Wsc2 and Wsc3 are paralogs with completely identical function (31). Since *P. pastoris* Wsc2 and Wsc3 display a much lower homology, their function may not overlap, which is why Wsc2 might simply not be expressed under the examined conditions.
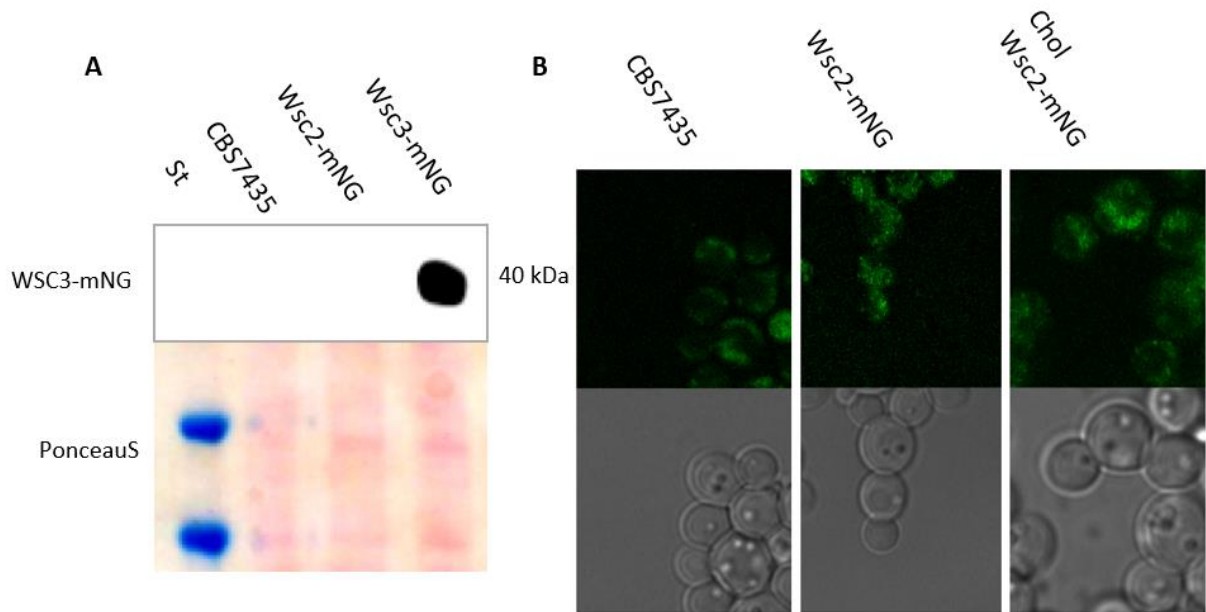
Figure 7: **Wsc2 is expressed at lower levels than Wsc3.** (A) Immunoblot analysis of wild type (CBS7435) and otherwise isogenic strains expressing Wsc2-mNG (yLB130) and Wsc3-mNG (yLB133). Cells were grown in YPD at 28°C for 16 h, harvested, lysed, and total cell lysates resolved by SDS–PAGE, and analysed by immunoblotting with anti-HA antibody, as described under Materials and Methods. Loading control, PonceauS. (B) Wild type (CBS7435) and otherwise isogenic strains expressing Wsc2-mNG (yLB130) and CBS7435 cholesterol Wsc3-mNG (yLB136)were grown in MD media at 28°C to a final OD$_{600}$ of 2, collected by brief centrifugation, and viewed by fluorescence microscopy (top panels) and bright field microscopy (bottom panels), as described under Materials and Methods.

To additionally confirm that fluorescent tagging does not harm functional expression of Wsc2 and Wsc3, hyperphosphorylation of Pim1 was checked in respective strains, but no difference could be observed (Figure 8).
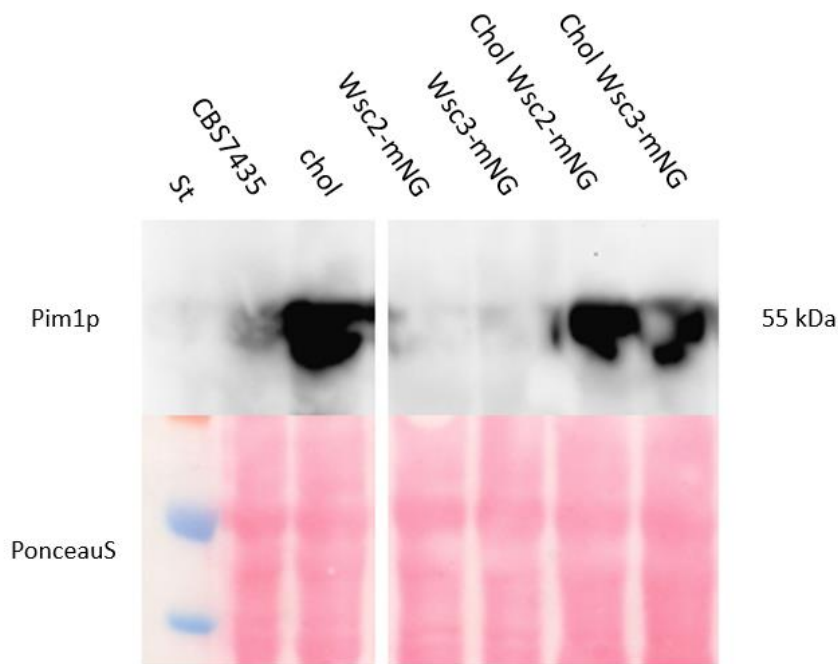
Figure 8: **Fluorescent tagging of Wsc proteins does not disturb Pim1 hyperphosphorylation.** Wild type cells (CBS7435), otherwise isogenic strains expressing Wsc2-mNG (yLB130) and Wsc3-mNG (yLB133), as well as CBS7435 strains producing cholesterol (MH458) and otherwise isogenic strains expressing Wsc2-mNG (yLB136) and Wsc3-mNG (yLB139) were grown for 40 h at 28°C, harvested, and lysed. Total cell lysates were resolved by SDS–PAGE and analysed by immunoblotting with anti-phospho-p44/42 antibody, as described under Materials and Methods. Loading control, PonceauS.

Wsc3 accumulates in cholesterol producing strains

To also investigate cellular localization and abundance of Wsc3, we imaged Wsc3-mNG in wild type and cholesterol producing strains. Similar to Wsc1 in *S. cerevisiae* (3), Wsc3 formed dot-like structures in the plasma membrane (PM). Interestingly, Wsc3 accumulated at the cellular periphery in cells producing cholesterol, which became very clear when we imaged cells at their top- and mid-section (Figure 9A). Automated signal quantification revealed that Wsc3-mNG signals increased 1.7- fold in cells producing cholesterol instead of ergosterol (Figure 9B).
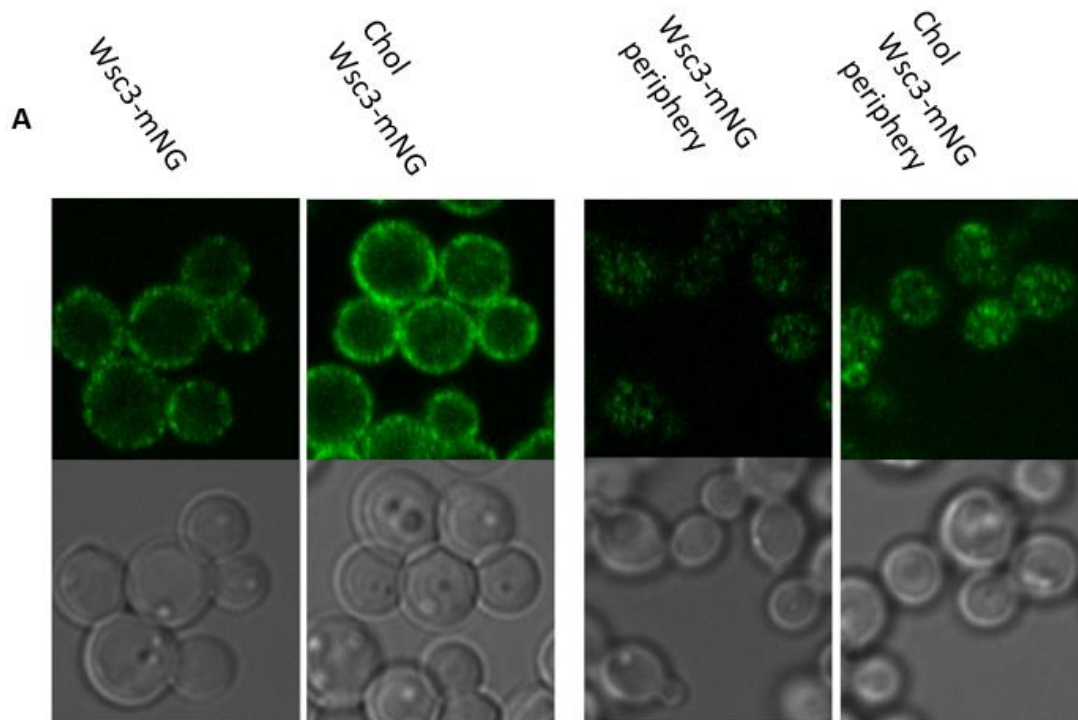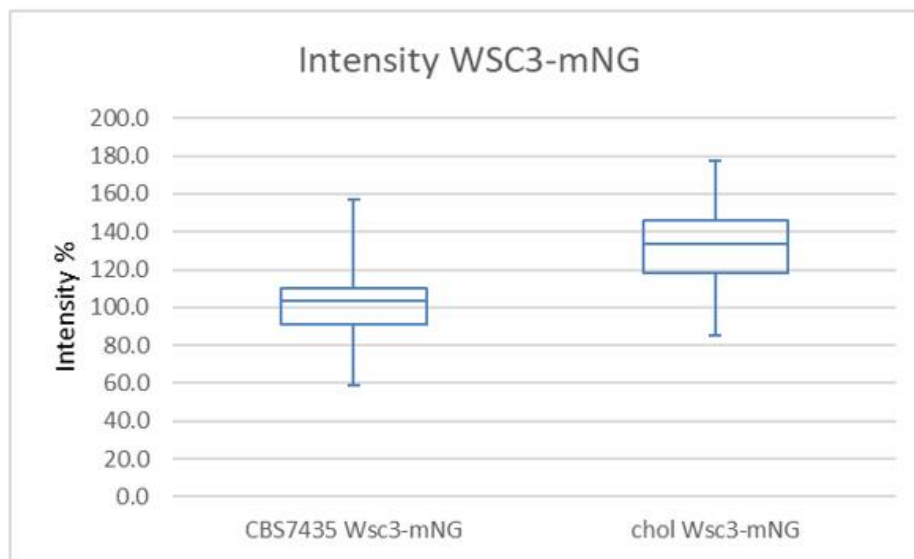
Figure 9: **Wsc3 accumulates at the plasma membrane of cells producing cholesterol.** (A) Wild type cells (CBS7435), expressing Wsc3-mNG (yLB133) and   cholesterol producing CBS7435 expressing Wsc3-mNG (yLB139) were grown in minimal media up to OD_{600} of 2 at 28°C, collected by brief centrifugation, and viewed by fluorescence microscopy (top panels) and bright field microscopy (bottom panels), as described under Materials and Methods. Cells were imaged at their top (images on the left) and mid-section (images on the right). (B) For the cell samples in A, PM-localized fluorescence was quantified (n > 40 cells each) using CellProfiler, and the values obtained were plotted in box-and-whisker format. Box represents the interquartile range (IQR) between lower quartile (25%) and upper quartile (75%); horizontal line represents the median value; whisker ends represent the lowest and highest data points still within 1.5 IQR of the lower and upper quartiles, respectively. For wild type cells expressing Wsc3-mNG, the initial median fluorescence intensity value at the PM was set to 100%.

Immunoblot analysis confirmed the results obtained by fluorescence microscopy, whereas overall protein concentrations of Wsc3-mNG even increased up to 5-fold in the cholesterol producing strain (Figure 10). This discrepancy could be explained by the fact that immunoblot analysis is a more holistic approach to quantify overall protein contents in a cell, whereas fluorescence signal intensities have only been quantified in the plasma membrane (Figure 9). Also, for immunoblot analysis, cells were grown in YPD medium, whereas minimal medium was used to grow cells for fluorescence microscopy, which might also have an impact on cellular protein contents. And last but not least, our imaging setup may not perfectly reflect actual protein concentrations, since the ratio between the photons emitted from a sample and the signal detected is not perfectly linear (32).

The real question is, why Wsc3 accumulates in the plasma membranes of cholesterol producing strains and how this is linked to the observed changes in cell wall morphologies. It has been reported that endocytosis of the pheromone receptor Ste2 is slowed down in cholesterol producing *S. cerevisiae* (33). Furthermore, it has been shown that *S. cerevisiae* expressing Wsc1 mutants defective in endocytosis not only accumulate Wsc1 at the PM but display slightly thickened cell wall structures and disturbed response to cell wall stressors (5). Hence, it seems highly likely that Wsc3 needs to directly interact with ergosterol for proper endocytosis. In case of abnormal sterol structures, Wsc3 may accumulate, and this accumulation may result in proportional activation and upregulation of the CWI pathway. To the same effect, it could be possible that Wsc3 even acts as sterol sensor through direct molecular interaction. It is known that disturbed sterol biosynthesis harms the stability and increases permeability of the plasma membrane (16). Hence, it seems possible that the cell senses modifications in sterol compositions by Wsc3 and counteracts by upregulating cell wall biosynthesis to additionally strengthen the cellular envelope.
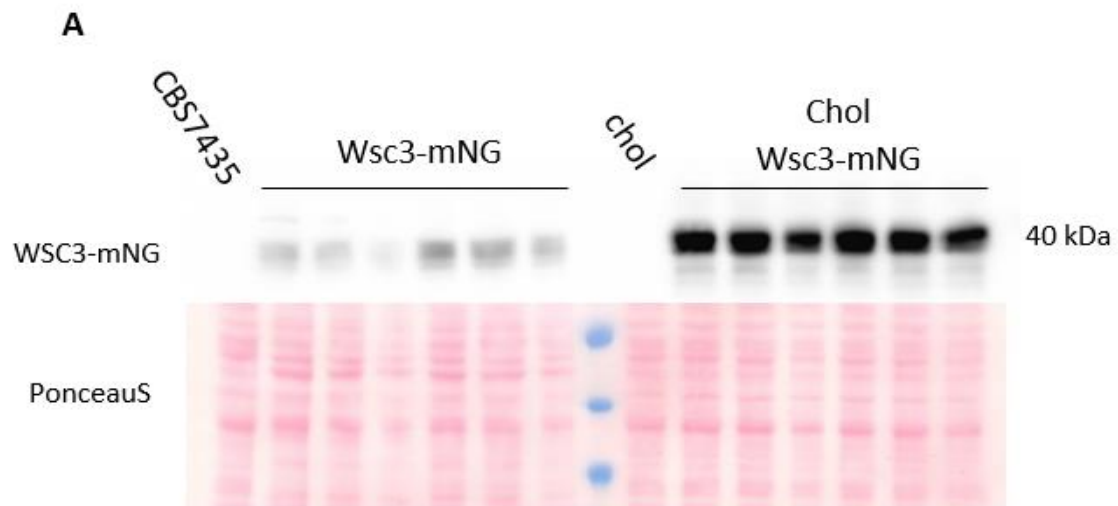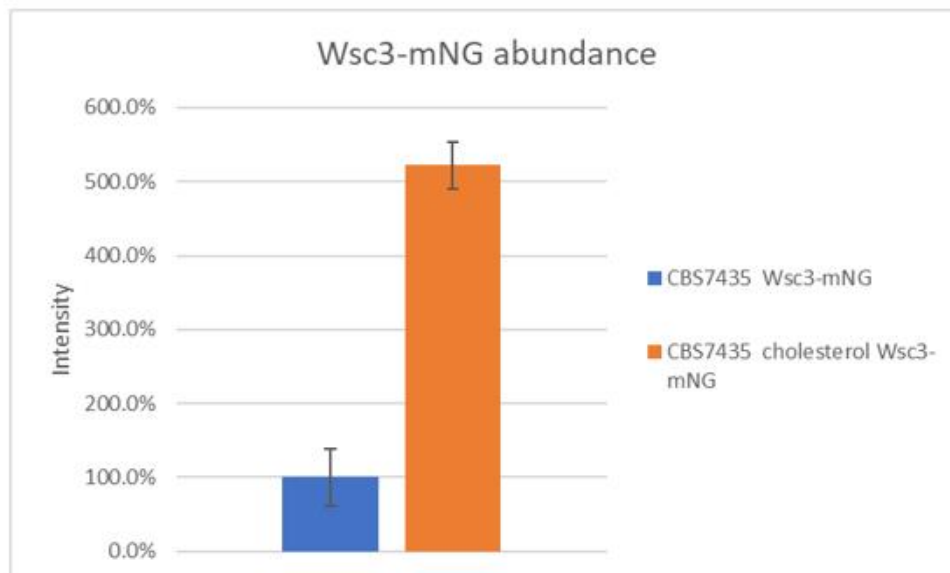
Figure 10: **Wsc3_mNG accumulates in cholesterol producing strains** (A) Immunoblot analysis of wild type (CBS7435) and otherwise isogenic strains expressing Wsc3-mNG (yLB133), as well as CBS7435 strains producing cholesterol (MH458) and otherwise isogenic strains expressing Wsc3-mNG (yLB139). Cells were grown in YPD at 28°C for 16 h, harvested, lysed, and total cell lysates resolved by SDS–PAGE, and analysed by immunoblotting with anti-HA antibody, as described under Materials and Methods. Loading control, PonceauS. (B) Intensities of bands in (A) were quantified via Fiji software. The mean intensity of all bands was blotted in percent of the mean intensity of CBS7435 expressing Wsc3-mNG (yLB133) (Data in *Table S 8*).

Conclusion and Outlook

In order to identify, which mechanisms are involved in responding to sterol changes and cause an upregulation of cell wall biosynthesis, we investigated CWI proteins Wsc1, Wsc2 and Wsc3. Studies using *S. cerevisiae* have shown that CWI proteins are membrane bound proteins, that react to cell wall stress and regulate transcription of a broad set of genes involved in cell wall biosynthesis, by initiating a MAPK cascade. Studies of *wsc1Δ* and *wsc2Δ wsc3Δ* knockout strains did neither reveal a clear phenotype in spot assays, nor lead to changes of CWI pathway activation as investigated by Pim1 phosphorylation. Our attempts to generate a triple knockout mutant failed, which suggests that the strain is most likely inviable, but further experimental proof has to be provided.

Through fluorescent and epitope tagging of Wsc2, we could show that the gene is barely expressed in both, the wild type and the cholesterol producing strain. However, by looking at Wsc3-mNG, it became clear that Wsc3 accumulates in the plasma membranes of cholesterol producing cells. It seems highly likely that this accumulation triggers upregulation of the CWI pathway; the molecular mechanisms, however, still have to be clarified. Thorough investigation of these mechanisms is currently in progress. Also, the role of Wsc1 in responding to sterol modifications will be examined.

References

1. Klis FM, Brul S, De Groot PWJ. Covalently linked wall proteins in ascomycetous fungi. Vol. 27, Yeast. 2010. p. 489–93.

2. Levin DE. Regulation of cell wall biogenesis in Saccharomyces cerevisiae: The cell wall integrity signaling pathway. Genetics. 2011 Dec;189(4):1145–75.

3. Rodicio R, Heinisch JJ. Together we are strong - Cell wall integrity sensors in yeasts. Vol. 27, Yeast. 2010. p. 531–40.

4. Zu T, Verna J, Ballester R. Mutations in WSC genes for putative stress receptors result in sensitivity to multiple stress conditions and impairment of Rlm1-dependent gene expression in Saccharomyces cerevisiae. Mol Genet Genomics [Internet]. 2001 Sep [cited 2020 Jan 15];266(1):142–55. Available from: http://www.ncbi.nlm.nih.gov/pubmed/11589572

5. Piao HL, Machado IMP, Payne GS. NPFXD-mediated endocytosis is required for polarity and function of a yeast cell wall stress sensor. Mol Biol Cell [Internet]. 2007 Jan [cited 2020 Jan 14];18(1):57–65. Available from: http://www.ncbi.nlm.nih.gov/pubmed/17065552

6. Levin DE. Cell Wall Integrity Signaling in Saccharomyces cerevisiae. Microbiol Mol Biol Rev. 2005 Jun 1;69(2):262–91.

7. Kimata Y, Ishiwata-Kimata Y, Yamada S, Kohno K. Yeast unfolded protein response pathway regulates expression of genes for anti-oxidative stress and for cell surface proteins. Genes to Cells. 2006 Jan;11(1):59–69.

8. Baumann K, Adelantado N, Lang C, Mattanovich D, Ferrer P. Protein trafficking, ergosterol biosynthesis and membrane physics impact recombinant protein secretion in Pichia pastoris. Microb Cell Fact. 2011 Nov 3;10.

9. Baumann K, Carnicer M, Dragosits M, Graf AB, Stadlmann J, Jouhten P, et al. A multi-level study of recombinant Pichia pastoris in different oxygen conditions. BMC Syst Biol. 2010 Oct 22;4.

10. Kock C, Dufrêne YF, Heinisch JJ. Up against the wall: Is yeast cell wall integrity ensured by mechanosensing in plasma membrane microdomains? Vol. 81, Applied and Environmental Microbiology. American Society for Microbiology; 2015. p. 806–11.

11. Cosano IC, Martín H, Flández M, Nombela C, Molina M. Pim1, a MAP kinase involved in cell wall integrity in Pichia pastoris. Mol Genet Genomics. 2001;265(4):604–14.

12. Dufourc EJ. Sterols and membrane dynamics. J Chem Biol. 2008 Nov;1(1–4):63–77.

13. Simons K, Ehehalt R. Cholesterol, lipid rafts, and disease. J Clin Invest [Internet]. 2002 Sep 1 [cited 2020 Jan 15];110(5):597–603. Available from:

http://www.jci.org/articles/view/16390

14. Beck JG, Mathieu D, Loudet C, Buchoux S, Dufourc EJ. Plant sterols in "rafts": A better way to regulate membrane thermal shocks. FASEB J. 2007 Jun;21(8):1714–23.

15. Schaller H. The role of sterols in plant growth and development. Vol. 42, Progress in Lipid Research. 2003. p. 163–75.

16. Hirz M, Richter G, Leitner E, Wriessnegger T, Pichler H. A novel cholesterol-producing Pichia pastoris strain is an ideal host for functional expression of human Na,K-ATPase α3β1 isoform. Appl Microbiol Biotechnol. 2013 Nov;97(21):9465–78.

17. Hirz M. Tuning of Pichia pastoris for the Expression of Membrane Proteins and Small Peptides. Technische Universität Graz; 2017.

18. Gibson DG, Young L, Chuang RY, Venter JC, Hutchison CA, Smith HO. Enzymatic assembly of DNA molecules up to several hundred kilobases. Nat Methods. 2009;6(5):343–5.

19. Lin-Cereghino J, Wong WW, Xiong S, Giang W, Luong LT, Vu J, et al. Condensed protocol for competent cell preparation and transformation of the methylotrophic yeast Pichia pastoris. Biotechniques. 2005;38(1):44–8.

20. Lõoke M, Kristjuhan K, Kristjuhan A. Extraction of genomic DNA from yeasts for PCR-based applications. Biotechniques. 2011 May;50(5):325–8.

21. Ahmad M, Winkler CM, Kolmbauer M, Pichler H, Schwab H, Emmerstorfer-Augustin A. *Pichia pastoris* protease-deficient and auxotrophic strains generated by a novel, user-friendly vector toolbox for gene deletion. Yeast [Internet]. 2019 Jul 30 [cited 2020 Jan 27];yea.3426. Available from: https://onlinelibrary.wiley.com/doi/abs/10.1002/yea.3426

22. Quail MA, Kelly SL. The extraction and analysis of sterols from yeast. Vol. 53, Methods in molecular biology (Clifton, N.J.). 1996. p. 123–31.

23. Ott RG, Athenstaedt K, Hrastnik C, Leitner E, Bergler H, Daum G. Flux of sterol intermediates in a yeast strain deleted of the lanosterol C-14 demethylase Erg11p. Biochim Biophys Acta - Mol Cell Biol Lipids. 2005 Jul 15;1735(2):111–8.

24. Schindelin J, Arganda-Carreras I, Frise E, Kaynig V, Longair M, Pietzsch T, et al. Fiji: An open-source platform for biological-image analysis. Vol. 9, Nature Methods. 2012. p. 676–82.

25. Jones TR, Kang IH, Wheeler DB, Lindquist RA, Papallo A, Sabatini DM, et al. CellProfiler Analyst: data exploration and analysis software for complex image-based screens. BMC Bioinformatics [Internet]. 2008 Nov 15 [cited 2020 Jan 28];9:482. Available from: http://www.ncbi.nlm.nih.gov/pubmed/19014601

26. Te Welscher YM, Ten Napel HH, Balagué MM, Souza CM, Riezman H, De Kruijff

B, et al. Natamycin blocks fungal growth by binding specifically to ergosterol without permeabilizing the membrane. J Biol Chem. 2008 Mar 7;283(10):6393–401.

27. Küberl A, Schneider J, Thallinger GG, Anderl I, Wibberg D, Hajek T, et al. High-quality genome sequence of Pichia pastoris CBS7435. J Biotechnol. 2011 Jul 20;154(4):312–20.

28. Näätsaari L, Mistlberger B, Ruth C, Hajek T, Hartner FS, Glieder A. Deletion of the pichia pastoris ku70 homologue facilitates platform strain generation for gene expression and synthetic biology. PLoS One. 2012 Jun 29;7(6).

29. Leskoske KL, Roelants FM, Emmerstorfer-Augustin A, Augustin CM, Si EP, Hill JM, et al. Phosphorylation by the stress-activated MAPK Slt2 down-regulates the yeast TOR complex 2. Genes Dev. 2018 Dec 1;32(23–24):1576–90.

30. Shaner NC, Lambert GG, Chammas A, Ni Y, Cranfill PJ, Baird MA, et al. A bright monomeric green fluorescent protein derived from Branchiostoma lanceolatum. Nat Methods. 2013 May;10(5):407–9.

31. Sekiya-Kawasaki M, Abe M, Saka A, Watanabe D, Kono K, Minemura-Asakawa M, et al. Dissection of upstream regulatory components of the Rho1p effector, 1,3-β-glucan synthase, in Saccharomyces cerevisiae. Genetics. 2002 Oct 1;162(2):663–76.

32. Bigio IJ, Fantini S. Quantitative Biomedical Optics: Theory, Methods, and Applications [Internet]. Cambridge University Press. 2016 [cited 2020 Jan 17]. 698 p. Available from: https://books.google.be/books?id=X7AkCwAAQBAJ&pg=PA19&dq=bulk+optic al+properties+tissues&hl=es&sa=X&ved=0ahUKEwjbkJGz_p3iAhUhWxUIHbJ GD9oQ6AEIMDAB#v=onepage&q=bulk optical properties tissues&f=false

33. Morioka S, Shigemori T, Hara K, Morisaka H, Kuroda K, Ueda M. Effect of sterol composition on the activity of the yeast G-protein-coupled receptor Ste2. Appl Microbiol Biotechnol. 2013 May 1;97(9):4013–20.

Appendix

Instruments and devices

Table S 1: **Instruments and devices**

Task	Instrument	Manufacturer
Absorbance measurement	Semi-Micro-Cuvettes, PS, 10 x 10 x 45 mm	Greiner bio-one AG, Germany
	BioPhotometer Plus	Eppendorf, Germany
	Microplate, 96-well, PS, U-bottom	Greiner bio-one AG, Germany
	SynergyMx	BioTek Instruments, USA
Agarose gel electrophoresis	PowerPac^{TM} Basic + Sub-Cell GT	Bio-Rad, USA
Centrifugation	Microcentrifuge 5415R	Eppendorf, Germany
	Tabletop centrifuge 5810R	Eppendorf, Germany
	Avanti^{TM} centrifuge, JA-10 rotors	Beckman Coulter^{TM}, USA
Determination of protein concentration	NanoDrop 2000 UV-Vis Spectrophotometer	Thermo Scientific, USA
Electrotransformation	MicroPulser^{TM}	Bio-Rad, USA
	Electroporation Cuvettes (2 mm gap)	Life Technologies, USA
Magnetic stirrer	IKAMAG RCT	IKA, Germany
Incubator (30°C and 37°C)	BINDER Kühlbrutschränke	Binder Gmbh, Germany
Mixing (small volumes)	Vortex – Genie 2	Scientific Industries Inc., USA
PCR reaction	GeneAmp® PCR System 2700	Applied Biosystems, USA
pH measurements	inoLab WTW 720 pH meter	WTW Gmbh, Germany
Protein electrophoresis	Mini Gel Tank	Thermo Scientific, USA

	NuPage® Novex® 4-12% Bis-Tris Mini Gels 1.0 mm, 15 wells	Life Technologies, USA
Shaker (small volumes)	Thermomixer comfort	Eppendorf, Germany
Shaker for cell cultivation	Multitron Standard	Infors AG, Switzerland
Sterile work	UNIFLOW KR130 biowizard	UNIQUIP, USA
Weighing	Lab scale: SI-202 Precision scale: Kern Scale ABS 220-4	Denver Instruments, USA Kern & Sohn Gmbh, Germany

Reagents

Table S 2: **Reagents**

Reagent	Manufacturer
Acetic acid	Roth GmbH, Germany
Agar Agar	Roth GmbH, Germany
Agarose LE	Biozyme, Germany
Ampicillin	Sigmar-Aldrich, Germany
Geneticin	Sigmar-Aldrich, Germany
Calcofluor-white	Roth GmbH, Germany
Natamycin	Koninklijke DSM N.V., Netherlands
Bovine Serum Albumin	Roth GmbH, Germany
Aqua bidest.	Fresenius Kabi GmbH, Austria
Ethanol	Roth GmbH, Germany
Ethidium bromide	Roth GmbH, Germany
Ethyl acetate	Roth GmbH, Germany
D-Glucose	Roth GmbH, Germany
DNA Loading dye (6x)	Thermo Scientific, USA

GeneRuler™ 1kb DNA Ladder	Thermo Scientific, USA
SDS	Roth GmbH, Germany
Lithiumacetate	Roth GmbH, Germany
Pyrogallol	Roth GmbH, Germany
Kalium hydroxide	Roth GmbH, Germany
n-heptane	Roth GmbH, Germany
Methanol	Roth GmbH, Germany
pyridine	Roth GmbH, Germany
N,O-bis(trimethylsilyl)-trifluoroacetamide	Sigma-Aldrich, Germany
NuPage LDS Sample Buffer (4x)	Life Technologies, USA
β-mercaptoethanol	Roth GmbH, Germany
Tris	Roth GmbH, Germany
Tween® 20	Roth GmbH, Germany
PageRuler™ Prestained Protein ladder	Thermo Scientific, USA
Trichloroacetic acid	Roth GmbH, Germany
Sodium chloride	Roth GmbH, Germany
Glass beads (d: 0.25-0.5 mm)	Roth GmbH, Germany
Peptone	Becton, Dickinson and Company; USA
Yeast extract	Becton, Dickinson and Company; USA
Yeast nitrogen base (YNB)	Becton, Dickinson and Company; USA
PEG	Roth GmbH, Germany
Biotin	Roth GmbH, Germany
Potassium chloride	Roth GmbH, Germany
Enzymes and adequate buffers, various	Thermo Scientific, USA

Buffer and media

Table S 3: **Buffer and media**

Name	Composition
SOB medium	20 g peptone, 5 g yeast extract, 0.59 g NaCl, 0.19 g KCl, 10 mM $MgSO_4$, 10 mM $MgCl_2$ dissolved in 1 L ddH_2O
SOC medium	20 g peptone, 3.46 g dextrose, 5 g yeast extract, 0.59 g NaCl, 0.19 g KCl, 10 mM $MgSO_4$, 10 mM $MgCl_2$ dissolved in 1 L ddH_2O
YPD medium	10 g Yeast extract, 20 g peptone, 20 g dextrose in 1 L ddH_2O
MD – His medium	13.4 g YNB, 20 g dextrose, $4x\ 10^{-5}$ % biotin in 1 L ddH_2O
Agar plates	20 g agar per Liter medium
TBS (10x)	30.3 g Tris, 87,6 g NaCl in 1 L ddH_2O adjust pH to 7.5 with HCl
TBST	900 mL ddH_2O +100 mL TBS (10x) + 0.3 mL Tween® 20
Transfer buffer	7.2 g Glycin, 1.45 g Tris in 900 mL ddH_2O + 100 mL methanol
Buffer A	4.8 g Tris in 1 L ddH_2O adjust pH to 7.5

Kits and enzymes

Table S 4: **Kits and enzymes used in this study**

Enzyme/Kit	Supplier
Fast Digest^{Tm} restriction enzymes	Thermo Scientific, USA
Phusion® DNA Polymerase	Sigma-Aldrich, Germany
Restriction enzymes	Thermo Scientific, USA

Taq DNA Polymerase	Thermo Scientific, USA
Gene Jet™ Plasmid Miniprep Kit	Thermo Scientific, USA
Wizard® SV Gel and PCR Clean Up System	Promega Corporation, USA
BCA™ Protein Assay Kit	Thermo Scientific, USA

Plasmids
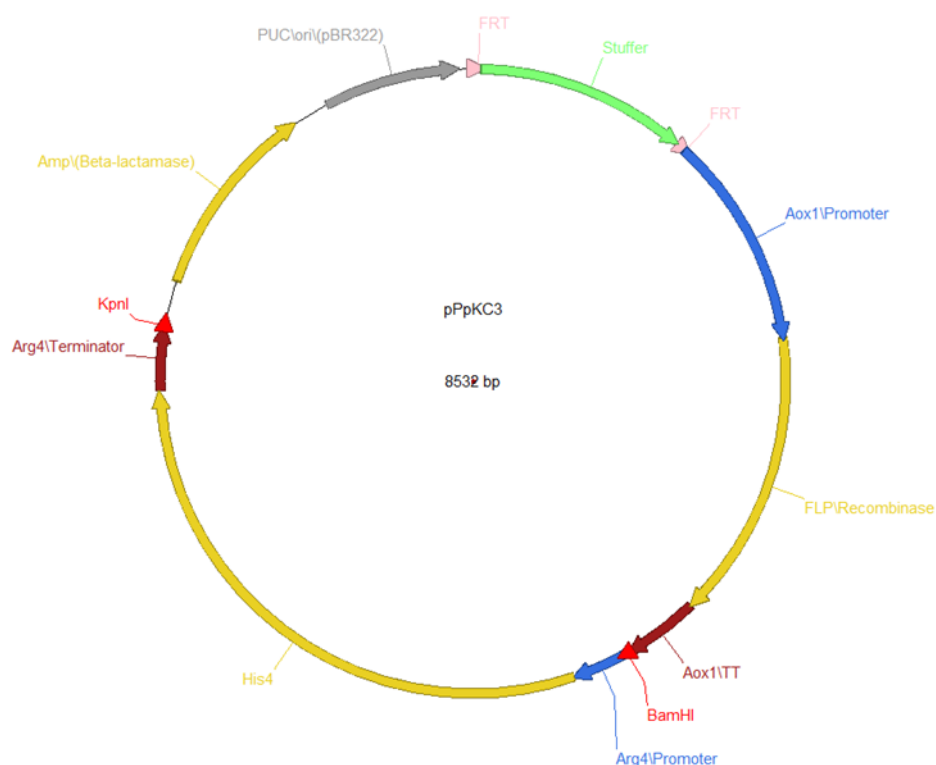
Figure S 1: **Schematic representation of the pPpKC3 vector.** It includes the *HIS4* gene for the selection in *P. pastoris,* flanked by restriction enzyme sites for KpnI and BamHI and and ampicillin resistance for selection in *E. coli.* It further includes an origin of replication for *E. coli,* a stuffer fragment and a recombinase flanked by a promotor and terminator from the yeast *AOX1* gene (21).

Figure S 2: **Schematic representation of the cassettes used for the fluorescence tagging of *WSC3 and WSC2* (A) and for the knock-out of all *WSC* genes (B).**
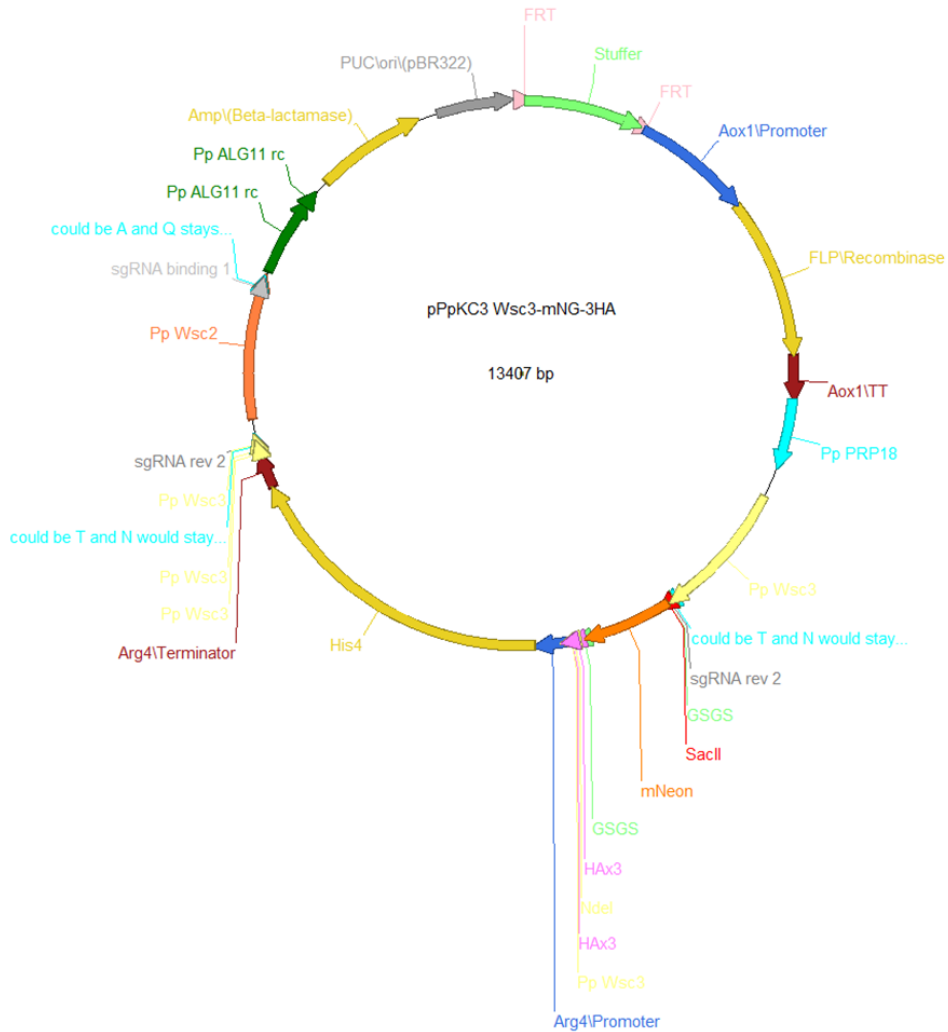
Figure S 3: **Schematic representation of the modified pPpKC3 vector used to tag W*SC3* with mNeonGreen**

Figure S 4: **Schematic representation of the modified pPpKC3 vector used to knock-out *WSC2* and *WSC3***

Primers

Table S 5: **Primers used in this study**

Primer	Target	Sequence
Fw1 (Wsc1)	*P. pastoris* genome	GAAGATTAAGTGAGACCTTCGTTCGTTTGTG CGGATCCATTTAAATCTTTTTTGAAAGGGTTC ATC
Rv1 (Wsc1)	*P. pastoris* genome	TCGCACAACCATGCTAAGATACGTTCCGTTC CGTTCCGGATCCGACTTCCTGACTCTGGGG
Fw2 (Wsc1)	pPpKC3	CCCCAGAGTCAGGAAGTCGGATCCGGAACG GAACGGAACGTATC
Rv2 (Wsc1)	pPpKC3	GCTACCCGTAACACCTTCCTGGAGTAATCTG CTTGGTACCAATGCGAGGATGCTG

Fw3 (Wsc1)	*P. pastoris* genome	ATCGTCTCCAGCAGCATCCTCGCATTGGTAC CAAGCAGATTACTCCAGGAAGGTG
Rv3 (Wsc1)	*P. pastoris* genome	TAGGCGTATCACGAGGCCCTTTCGTCGGTA CCATTTAAATATGACGTCTCCATTCCG
Fw1 (Wsc2-3)	*P. pastoris* genome	GAAGATTAAGTGAGACCTTCGTTCGTTTGTG CGGATCCATTTAAATCAGTTCCATCACAATGT G
Rv1 (Wsc2-3)	*P. pastoris* genome	TCGCACAACCATGCTAAGATACGTTCCGTTC CGTTCCGGATCCGGTGTTTAAGTTCTCAGTA ATG
Fw2 (Wsc2-3)	pPpKC3	AAATCACATTACTGAGAACTTAAACACCGGA TCCGGAACGGAACGGAACGTATC
Rv2 (Wsc2-3)	pPpKC3	CTCAAAATCGTCATCTTGATCAAACCTTCTG GTACCAATGCGAGGATGCTG
Fw3 (Wsc2-3)	*P. pastoris* genome	ATCGTCTCCAGCAGCATCCTCGCATTGGTAC CAGAAGGTTTGATCAAGATGAC
Rv3 (Wsc2-3)	*P. pastoris* genome	TAGGCGTATCACGAGGCCCTTTCGTCGGTA CCATTTAAATCTTACAAACTAGTCATGATC
Fw(Wsc-mNG)	*S. cerevisiae* yAEA301 genome	GGTTCTGGATCCCCGCGGGTGAG
Rv(Wsc3-mNGa)	*P. pastoris* genome	TTATCCTCCTCGCCCTTGCTCACCCGCGGG GATCCAGAACCAACTTCATCATCTGTGGGG
Rv(Wsc3-mNGb)	*P. pastoris* genome	TCCGGATCCGGTGTTTAAGTTCTCAGTAATG TGATTTCTAAGCGTAATCTGGAACGTCGT
Rv(HIS4_Wsc3)	pPpKC3	GGTACCAATGCGAGGATGCT
Fw(Wsc3mNG_down)	*P. pastoris* genome	AACTTTGAATCGTCTCCAGCAGCATCCTCGC ATTGGTACCCCGGATGTAACTCAGGATAG
Rv(Wsc2-mNGa)	*P. pastoris* genome	CCTCCTCGCCCTTGCTCACCCGCGGGGATC CAGAACCAGTTGTTCCGAATGAATTTTCAC
Rv(Wsc2-mNG-short)	*P. pastoris* genome	AGTTGTTCCGAATGAATTTTCACTTG

Data

Table S 6: **Intensity of mNG in wt and cholesterol *P. pastoris* strains with mNG-tagged Wsc3.** As 100% intensity the mean intensity value of the wt cells was picked. Calculations were done with the values from *Table S 7*

	Intensity			Intensity %	
	wt	**chol**		**wt**	**chol**
mean	0.150	0.259		100.0	172.8
median	0.145	0.260		96.3	173.1
1. Quartil	0.136	0.227		90.9	151.3
3. Quartil	0.169	0.283		112.5	188.3
min	0.112	0.145		74.5	96.8
max	0.192	0.384		128.2	256.0

Table S 7: **Intensity values of Wsc3_mNG derived from fluorescence microscopy with a cellprofiler pipeline**

clone number	wt	chol
1	0.12046468	0.22896403
2	0.11561823	0.35882995
3	0.13836125	0.16645454
4	0.13036125	0.26195999
5	0.1119107	0.34372915
6	0.13760858	0.28352455
7	0.14452994	0.20551325
8	0.11744527	0.33588412
9	0.17477942	0.3016897
10	0.13495139	0.24139594
11	0.16954982	0.27103591
12	0.12630034	0.23655171
13	0.13222223	0.28473509
14	0.1629797	0.1453212
15	0.15761787	0.32704143
16	0.15131222	0.308541
17	0.14815353	0.277697

18	0.13906784	0.26487746
19	0.17307472	0.24950669
20	0.15994291	0.22028536
21	0.13535694	0.22657916
22	0.1370487	0.27387649
23	0.16932719	0.19827432
24	0.1540107	0.20240327
25	0.17335963	0.28176063
26	0.17376945	0.24842306
27	0.15275736	0.27738844
28	0.19242315	0.34560515
29	0.13643264	0.29464397
30	0.18543544	0.28289236
31	0.13837356	0.19845361
32	0.14421356	0.27805986
33	0.16530609	0.31964109
34	0.14461408	0.25159001
35	0.1364239	0.24085265
36	0.14353009	0.2253784
37	0.168539	0.25412233
38	0.18029231	0.21667122
39	0.17729938	0.20956062
40		0.26160858
41		0.20877876
42		0.26832168
43		0.28047168
44		0.19687686
45		0.3219464
46		0.27869919

47		0.23893667
48		0.24135777
49		0.25839596
50		0.23035231
51		0.26147232
52		0.38432826
53		0.20110903
54		0.23179698

Table S 8: **Intensity of immunoblot band signal in CBS7435 and cholesterol strains expressing mNG-tagged Wsc3.** Analysed by immunoblotting with anti-HA antibody and quantifying signal strenght via Fiji software. (*Figure 10*)

Intensity	
CBS7435 Wsc3-mNG	**chol Wsc3-mNG**
6,295,165.25	35,166,721.36
5,367,123.71	38,850,930.57
3,178,186.266	41,177,493.05
10,873,101.88	41,992,467.74
10,947,715.57	36,847,193.94
7,820,405.926	38,303,213.92